A Novel Real-time Edge-preserving Smoothing Filter

Simon Reich[1], Alexey Abramov[1], Jeremie Papon[1], Florentin Wörgötter[1] and Babette Dellen[2]
[1]*Third Institute of Physics - Biophysics, Georg-August-Universität Göttingen, Friedrich-Hund-Platz 1, 37077 Göttingen, Germany*
[2]*Institut de Robotica i Informatica Industrial (CSIC-UPC), Llorens i Artigas 4-6, 08028 Barcelona, Spain*

Keywords: Texture Filter, Image Segmentation, GPU, Real-time, Edge-preserving.

Abstract: The segmentation of textured and noisy areas in images is a very challenging task due to the large variety of objects and materials in natural environments, which cannot be solved by a single similarity measure. In this paper, we address this problem by proposing a novel edge-preserving texture filter, which smudges the color values inside uniformly textured areas, thus making the processed image more workable for color-based image segmentation. Due to the highly parallel structure of the method, the implementation on a GPU runs in real-time, allowing us to process standard images within tens of milliseconds. By preprocessing images with this novel filter before applying a recent real-time color-based image segmentation method, we obtain significant improvements in performance for images from the Berkeley dataset, outperforming an alternative version using a standard bilateral filter for preprocessing. We further show that our combined approach leads to better segmentations in terms of a standard performance measure than graph-based and mean-shift segmentation for the Berkeley image dataset.

1 INTRODUCTION

The segmentation of image areas into perceptually uniform parts continues to be a challenging computer-vision problem due to the large variety of textures and materials in our natural environment. Another important issue is the performance of the methods in terms of computation time. Many applications would profit largely from a real-time segmentation method that is able to handle a broad spectrum of different images.

When grouping image areas into segments a similarity criterion needs to be defined. However, similarities can exist on different scales, i.e., between adjacent pixels, or groups of pixels, as it is the case for texture. Segmentation algorithms thus need to take into account similarities occurring at these different scales, which can be rather costly. Graph-based segmentation algorithms solve this problem through the definition of an adaptive similarity measure, which depends on the average pixel-to-pixel similarity inside growing regions (Felzenszwalb and Huttenlocher, 2004). The mean-shift segmentation algorithm by (Comaniciu and Meer, 2002) performs a non-parametric analysis in the feature space (Paris and Durand, 2007) by iteratively computing average values of pixels inside a Gaussian neighborhood. Through this process, feature values of pixels are successively moved towards the mean value of a local neighborhood. Upon convergence of the procedure, the feature values are grouped using a clustering method. While providing quite satisfactory results, both methods have the disadvantage that they are based on a sequential process, and thus are not readily parallizable, limiting their performance.

Alternatively, the image can be pre-processed using a smoothing filter for homogenizing textured areas and making them this way workable for standard segmentation and clustering methods. During the past two decades many types of smoothing filters have been proposed. Most filters are based on two basic steps: first detecting noise and second removing it. In noise detection, noise and noise-free areas are distinguished using a threshold. These thresholds can be either learned using a training set of images, as in support vector machines (Yang et al., 2010) and neural networks (Muneyasu et al., 1995), or the threshold may be computed from the surrounding pixel values, as in (Du et al., 2011). (Lev et al., 1977) identified similar pixels by detecting edges and iteratively replacing the intensity of the pixel by the mean of all pixels in a small environment. Another approach was proposed by (Tomasi and Manduchi, 1998). The bilateral filter blurs neighboring pixels depending on their combined color and spatial distance. Hence,

Reich S., Abramov A., Papon J., Wörgötter F. and Dellen B..
A Novel Real-time Edge-Preserving Smoothing Filter.
DOI: 10.5220/0004214300050014
In *Proceedings of the International Conference on Computer Vision Theory and Applications* (VISAPP-2013), pages 5-14
ISBN: 978-989-8565-47-1

only texture which has a small deviation from the mean can be blurred without affecting boundaries. This leads to a trade-off for highly textures area: Large blurring factors are needed to smooth out texture, having the consequence that edges are not preserved anymore.

In the current work, we present a novel smoothing filter which is not limited by these constraints. The basic idea can be described as follows: Given a measurement window, the feature values of the pixel values inside the window are smoothed with a smoothing factor dependent on the window size. If smoothing decreased the distance from the average value below a certain threshold, all pixels in the window are replaced by their smoothed value and a component that depends on the average value. If smoothing does not decrease the distance from the mean sufficiently, it is assumed that a true boundary is located inside the window, and the original feature values are kept. This procedure is repeated for many different window locations and sizes (optional). Since the procedures for each window are independent from each other, the algorithm can be easily parallelized. We show in this paper that the proposed filter leads to improved segmentations in conjunction with a recent real-time segmentation algorithm based on the superparamagnetic clustering of data (Abramov et al., 2012), and outperforms the bilateral filter on the Berkeley database. Importantly, the filter runs in real time on a GPU, providing a powerful add-on to the existing segmentation technique, which can also be applied to video segmentation. We further compare our results to the graph-based and the mean-shift segmentation on the Berkeley segmentation dataset and benchmark (Martin et al., 2001).

While these segmentation algorithms are color-based, partitioning could also base on e.g. an object classification library as in (Farmer and Jain, 2005) or depth information as in (Cigla and Aydin Alatan, 2008). These algorithms need either a training phase, a set of fixed parameters or other pre-set information. Other than segmentation and image smoothing, texture and noise filters are found in many other applications including denoising (Elad, 2002; Jiang et al., 2003), tone management (Farbman et al., 2008; Durand and Dorsey, 2002), demosaicking (R. and W., 2003; Farsiu et al., 2006) or optical flow estimation (Xiao et al., 2006; Sun et al., 2010).

The paper is organized as follows. In section 2 we introduce the proposed filter and describe the processing flow. In section 3 we present obtained segmentation results and evaluate the performance of the method quantitatively. In section 4 we conclude our work.

2 APPROACH

2.1 Proposed Filter

A diagram of the proposed filter is given in figure 1. First the image Φ is divided into subwindows Ψ of the size $N = k \cdot l$. Each subwindow is shifted by one pixel relative to the last one, such that there are as many subwindows as there are pixels in the image. Then, the pixels inside each subwindow are smoothed. A distance $\delta_{i,j}$ for each pixel inside the subwindow and a mean distance δ_m are computed in the color domain to obtain a measurement for noise, as described below. A user selected value τ defines a threshold between noise or texture and a color edge. If noise is detected, a weight $\omega_{i,j}$ is calculated which moves the color values of the respective pixel towards the mean color of the subwindow.

1. Smoothing and Division into Subwindows. The image Φ holds the RGB color vectors $\boldsymbol{\varphi}_{i,j} = (\varphi^r_{i,j}\ \varphi^g_{i,j}\ \varphi^b_{i,j})^T$. Beginning in the upper left corner, the pixels $\boldsymbol{\varphi}_{i,j}$ to $\boldsymbol{\varphi}_{i+k,j+l}$ are copied into a subwindow Ψ of size $k \times l$ holding the color vectors $\boldsymbol{\psi}_{r,s}$. $(i\ j)^T$ is in the range of the image size, while $(r\ s)^T$ is in the range of the subwindow size $k \times l$. Each subwindow is smoothed using a Gaussian filter function to remove outliers which would distort the calculation of the mean as described below.

2. Computation of the Distance Matrix. The arithmetic mean of Ψ is calculated as

$$\boldsymbol{\psi}_m = \frac{1}{N}\left(\sum_{r,s}\psi^r_{r,s}\ \sum_{r,s}\psi^g_{r,s}\ \sum_{r,s}\psi^b_{r,s}\right)^T \tag{1}$$

where $N = k \cdot l$ denotes the size of the subwindow. The pixelwise distances

$$\delta_{r,s} = |\boldsymbol{\psi}_{r,s} - \boldsymbol{\psi}_m|_2, \tag{2}$$

as well as the resulting mean pixelwise distance for each subwindow Ψ, is computed to

$$\delta_m = \frac{1}{N}\sum_{r,s}\delta_{r,s}. \tag{3}$$

3. Thresholding. $\delta_{r,s}$ is now used for low level noise detection. Small scaled color variations will result in a low variance $\delta_{r,s}$ values since all color values are close to the mean color value. In case of a sharp color edge a large $\delta_{r,s}$ is obtained. Therefore, we can use a threshold τ to identify noisy pixels, yielding

$$\psi_{r,s} = \begin{cases} 1 & \delta_{r,s} \le \tau \quad \text{and} \quad \delta_{\mathrm{m}} \le \tau, \\ 0 & \text{else,} \end{cases} \tag{4}$$

where 1 stands for a noisy or textured pixel.

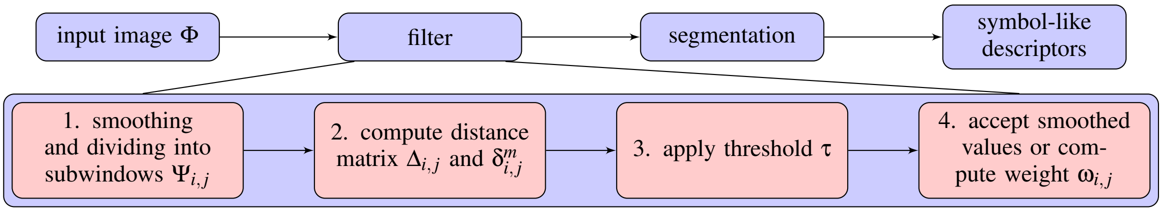

Figure 1: Schematic of the proposed filter.

4. Computation and Updating of RGB Values. At every iteration a global, image wide weight $\omega_{i,j}$ is computed for normalization. A subwindow wide weight, consisting of the squared distance of the user based threshold τ and the pixelwise distance $\delta_{r,s}$, is used for updating pixel values within one subwindow. Please note that due to the sliding subwindows each pixel gets updated $N = k \cdot l$ times. The global weight $\omega_{i,j}$ is initialized with zeros and updated according to

$$\omega_{i,j} \longleftarrow \omega_{i,j} + \psi_{r,s} \cdot (\tau - \delta_{r,s})^2, \tag{5}$$

where the $\omega_{i,j}$ define the matrix Ω. For the updated pixel values a third image frame Θ of the size of the original image is needed. Θ is initalized with zeros and updated according to

$$\boldsymbol{\theta}_{i,j} \longleftarrow \boldsymbol{\theta}_{i,j} + \psi_{r,s} \cdot (\tau - \delta_{r,s})^2 \cdot \boldsymbol{\psi}_m. \tag{6}$$

Again, every pixel value is updated N times. When the algorithm has reached the last iteration, all updated pixels Θ are added to the original image Φ and normalized using Ω. Even though it is highly improbable that any entry in Ω equals zero, 1 is added to every entry. As in general $\omega_{i,j} \gg 0$ and specifically $\omega_{i,j} \geq 0$ is true, this does not change the outcome significantly. This way the output is moved to the mean color value $\boldsymbol{\psi}_{\mathrm{m}}$. Two examples for subwindow arrays can be seen in figure 2(a) and 2(b) (grayscaled input subwindow on the left side, output subwindow on the right side). In figure 2(d) an example for noisy pixels in a subwindow is shown, which corresponds to the image in 2(a). The pixelwise distance as well as the mean pixelwise distance are below the threshold τ, and the pixel color values are shifted towards the mean color values. In figure 2(e) a noisy step function is shown, which relates to image 2(b). Here τ is smaller than the distances and the pixels are not updated to the mean value. Since we use sliding subwindows, the small scaled noise in pixels 0 to 4 and 5 to 9 will be corrected but the edge will be preserved.

2.2 Formulation of the Proposed Filter in the Continuous Domain

Let $\boldsymbol{f}(\boldsymbol{x})$ define the smoothed input image, $\boldsymbol{h}(\boldsymbol{x})$ the output image, $\boldsymbol{c}(\boldsymbol{\zeta}, \boldsymbol{x})$ measures the geometric closeness and $\boldsymbol{s}(\boldsymbol{f}(\boldsymbol{\zeta}), \boldsymbol{f}(\boldsymbol{x}))$ the photometric similarity. As we want to address specifically color images, bold letters refer to RGB-vectors. In this section $|\cdot|$ also refers to per-element-multiplication instead of vector multiplication. In our approach we first want to detect noise and texture based on a user defined parameter τ. If noise or texture is detected, we want to remove it, and in case of a color edge, we want to preserve the edge. Therefore, we define a mean value

$$\begin{aligned} \boldsymbol{m}(\boldsymbol{x}) &= \boldsymbol{k}_m^{-1}(\boldsymbol{x}) \int_{-\infty}^{\infty}\int_{-\infty}^{\infty} \boldsymbol{f}(\boldsymbol{\zeta}) \cdot \boldsymbol{c}(\boldsymbol{\zeta}, \boldsymbol{x})\, \mathrm{d}\boldsymbol{\zeta} \\ \boldsymbol{k}_m(\boldsymbol{x}) &= \int_{-\infty}^{\infty}\int_{-\infty}^{\infty} \boldsymbol{c}(\boldsymbol{\zeta}, \boldsymbol{x})\, \mathrm{d}\boldsymbol{\zeta} \end{aligned} \tag{7}$$

and a distance function

$$d(\boldsymbol{f}(\boldsymbol{x}), \boldsymbol{m}(\boldsymbol{x})) = |\boldsymbol{f}(\boldsymbol{x}) - \boldsymbol{m}(\boldsymbol{x})|, \tag{8}$$

which results in the pixelwise distance. The mean value $\boldsymbol{m}(\boldsymbol{x})$ now holds the average color value inside a spatial neighborhood of $\boldsymbol{x}$ and d holds the color distance from the pixel to the average $\boldsymbol{m}(\boldsymbol{x})$. If the spatial neighborhood holds only small scaled noise or texture we expect a low pixelwise distance d, as well as a low average pixelwise distance in the spatial neighborhood $\boldsymbol{c}$:

$$\begin{aligned} p(\boldsymbol{x}) &= k_p^{-1} \iint_{-\infty}^{\infty} d(\boldsymbol{f}(\boldsymbol{\zeta}), \boldsymbol{m}(\boldsymbol{x}))\, \boldsymbol{c}(\boldsymbol{\zeta}, \boldsymbol{x})\, \mathrm{d}\boldsymbol{\zeta} \\ k_p(\boldsymbol{x}) &= \iint_{-\infty}^{\infty} \boldsymbol{c}(\boldsymbol{\zeta}, \boldsymbol{x})\, \mathrm{d}\boldsymbol{\zeta}. \end{aligned} \tag{9}$$

Therefore, we can make a binary decision using a threshold τ as

$$\boldsymbol{h}(\boldsymbol{x}) = \boldsymbol{k}_R^{-1}(\boldsymbol{x}) \cdot \begin{cases} \iint_{-\infty}^{\infty} \boldsymbol{f}(\boldsymbol{\zeta}) \cdot \boldsymbol{c}(\boldsymbol{\zeta}, \boldsymbol{x}) \cdot \boldsymbol{s}(\boldsymbol{\zeta}, \boldsymbol{x})\, \mathrm{d}\boldsymbol{\zeta} & p,\, d \leq \tau \\ \iint_{-\infty}^{\infty} \boldsymbol{f}(\boldsymbol{\zeta}) \cdot \boldsymbol{c}(\boldsymbol{\zeta}, \boldsymbol{x})\, \mathrm{d}\boldsymbol{\zeta} & \text{else}, \end{cases} \tag{10}$$

where k_R is the respective normalization. We used a 2D step function

$$\boldsymbol{c}(\boldsymbol{\zeta}, \boldsymbol{x}) = \begin{cases} 1 & \boldsymbol{x} - \boldsymbol{a} \leq \boldsymbol{\zeta} \leq \boldsymbol{x} + \boldsymbol{b} \\ 0 & \text{else} \end{cases}, \tag{11}$$

using the conditions $\boldsymbol{a}, \boldsymbol{b}, \boldsymbol{e} \in \mathbb{R}^2_{\geq 0} | \boldsymbol{a} + \boldsymbol{b} = \boldsymbol{e}$ with a fixed $\boldsymbol{e}$. This generates a rectangle of the size $\boldsymbol{e}$ around $\boldsymbol{x}$. As this definition is not feasable in the continuous

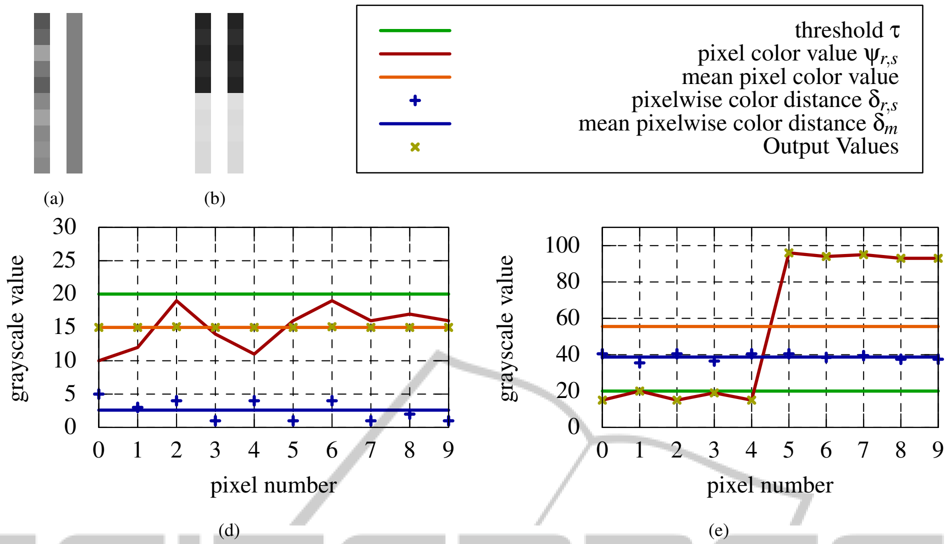

Figure 2: 2(a) Low level white noise (left) in 10 pixels is used as input for filtering. The right bar shows the same 10 pixels after filtering. The computational steps involved in this image can be seen in figure 2(d). 2(b) A noisy step function is used for input. After filtering input and output are indentical to preserve the edge. The computational steps are shown in figure 2(e). 2(d) The pixelwise and mean pixelwise distance are both below the threshold τ. The output is filtered according to (4) and moved to the mean color. 2(e) The pixelwise and mean pixelwise distance are above the threshold and the output is not filtered. The edge is therefore preserved.

domain as it generates a nonfinite number of subwindows to calculte, in the discrete case however every pixel is checked and updated according to its neighborhood $\boldsymbol{e}$. As a measure for similarity we used a squared distance

$$\boldsymbol{s}(\boldsymbol{x}) = (\tau - d(\boldsymbol{f}(\boldsymbol{x}), \boldsymbol{m}(\boldsymbol{x})))^2 |\boldsymbol{m}(\boldsymbol{x})| \qquad (12)$$

and the euclidian norm. In case of texture detection the output is moved to the mean. The maximum size of the step can be adjusted via the threshold τ.

2.3 Real-time Implementation

Real time can only be achieved by running the proposed technique on parallel hardware, because the computation of multiple subwindows is very intensive on traditional CPUs. Once the image Φ is read, values for the subwindows Ψ can be computed independently. For accelaration we use a graphics processor unit (GPU) and an example implementation can be seen in figure 3(a). One block on the GPU starts 32×16, and each of them loads one pixel into shared memory. Each thread calculates the pixelwise distances for one subwindow Ψ (marked red for two example threads). As shown in white several threads remain idle after copying. Since we are interested in the average noise, we chose periodic mirrored boundary conditions, which is illustrated in figure 3(b).

In our approach the images are filtered twice using subwindows of size $k = 8$, $l = 4$ and $k = 4$, $l = 8$. Two runs are used for symmetry purposes and better filter results. As Δ and δ_m are calculated over each subwindow, this also sets the maximum size of texture that is detected. We tested two implementations of the algorithm: The CPU measurement refers to a single-threaded implementation using an AMD Phenom 9550 quad-core processor at 2,2 GHz using one core and 4 GB RAM. The GPU version is executed on an Nvidia GTX580 graphics card using 512 cores and 1.5 GB device memory.

3 EXPERIMENTAL RESULTS

3.1 Filter Results

In figure 5 a visual comparison of different threshold levels is shown. Above a threshold of $\tau = 35$ the output does not change much, which is easily understood when looking at equation 4. Above a certain threshold level every pixel is identified as either noise or texture and smoothed out. Therefore, it is not necessary to adapt the user based threshold τ to different noise levels. As shown below, there is a best value for τ for non-artificial images.

Also in this work noise and texture is treated equally. But contrary to a denoising filter we do not want to restore a noisy image, but fill out large areas with small color variations using the mean color. This includes that noise, but also larger structures like

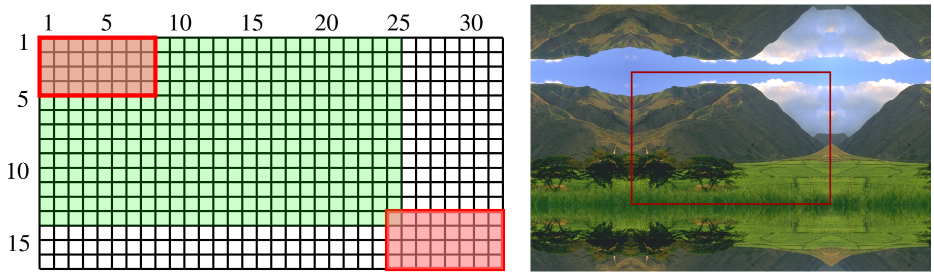

(a) (b)

Figure 3: 3(a) Example for parallelization on a GPU. One block loads 32×16 px into shared memory where each subwindow, shown in red, is computed by one thread. The next block would start at pixel 26. For the green pixels the weight ω will be updated. 3(b) We used periodic mirrored boundary conditions as it leads to a good representation of the average noise at the border.

texture, are smoothed out. As we are interested in the perception-action loop of robots and improvement of color-based segmentation results, the latter one is more important to the results.

In figure 4(a) we compare the proposed filter to a bilateral filter (Tomasi and Manduchi, 1998). As a bilateral filter only smoothes the image based on the spatial and color distance, it either does not preserve the edge, but smoothes the texture, or preserves the edge and does not filter the texture.

3.2 Segmentation Results

We filtered all images from the Berkeley Segmentation Dataset and Benchmark (Martin et al., 2001) using a large variety of different thresholds. Afterwards the filtered images were segmented and compared with the ground truth images from the database. The performance was evaluated using the precision and recall method following (Martin et al., 2004). Given an original image Φ, its machine segmentation S', and the corresponding ground truth S, precision is defined as the fraction of boundary pixels in the segmented image S' that also occur in the ground truth S over the total number of boundary pixels in S'. It is therefore sensitive to over-segmentation. Recall measures the fraction of boundary pixels in S which are also found in S'. It is sensitive to under-segmentation. The results shown are the arithmetic means of all values computed.

Figure 6(a) shows the precision and recall values for the Metropolis algorithm using constant segmentation parameters for various threshold values τ. Above a threshold of $\tau = 35$ the values remain steady. The weighted mean of precision and recall indicate that best results are obtained for a threshold of $\tau = 30$. This behavior was also observed using different segmentation parameters and may also be seen in the filtered images shown in figure 5. Also note that precision is considerably lower than recall. While the ideal value would be 1 for both, the segmented images are extremely rich on texture, resulting in over-segmentation. The threshold is computed using the Berkeley Segmentation Dataset and Benchmark which offers a wide range of heavily textured natural images. However, our experiments show that $\tau = 30$ may be considered a good value for all scenes offering good color contrast. As in low contrast scenes the color segmentation will most likely fail, we do not take it into further consideration.

In figure 6(b) we show the segmentations for different values of the parameter α_1 using the Metropolis algorithm. The parameter α_1 is a system parameter used to increase or decrease the coupling strength in the clustering model. Thus, it influences the total number of segments. Other parameters were taken from (Abramov et al., 2012). Best results in the trade-off between over- and under-segmentation were achieved for $\alpha_1 = 1.0$.

Next, we compare our method with the graph-based segmentation, mean-shift algorithm and an alternative version of the Metropolis algorithm using the standard bilateral filter for smoothing (see figure 6(c)). While the Metropolis algorithm without filter performs better than the graph-based and mean shift segmentation, precision is improved when using the proposed filter. Results are shown for different α_1 values for the Metropolis algorithm. The value for $\alpha_1 = 1.0$ is marked with a circle. For graph-based segmentation we used the combination of parameters recommended by the authors for segmentation of arbitrary images, see (Felzenszwalb and Huttenlocher, 2004). The mean shift algorithm of (Paris and Durand, 2007) uses three input parameters: the Gaussian parameters σ_c and σ_s for color and spatial domain respectively and the persistent threshold τ_p. We determined experimentally the combination $\sigma_c = 2$, $\sigma_s = 8$ and $\tau_p = 1$ for best results. On purpose, we

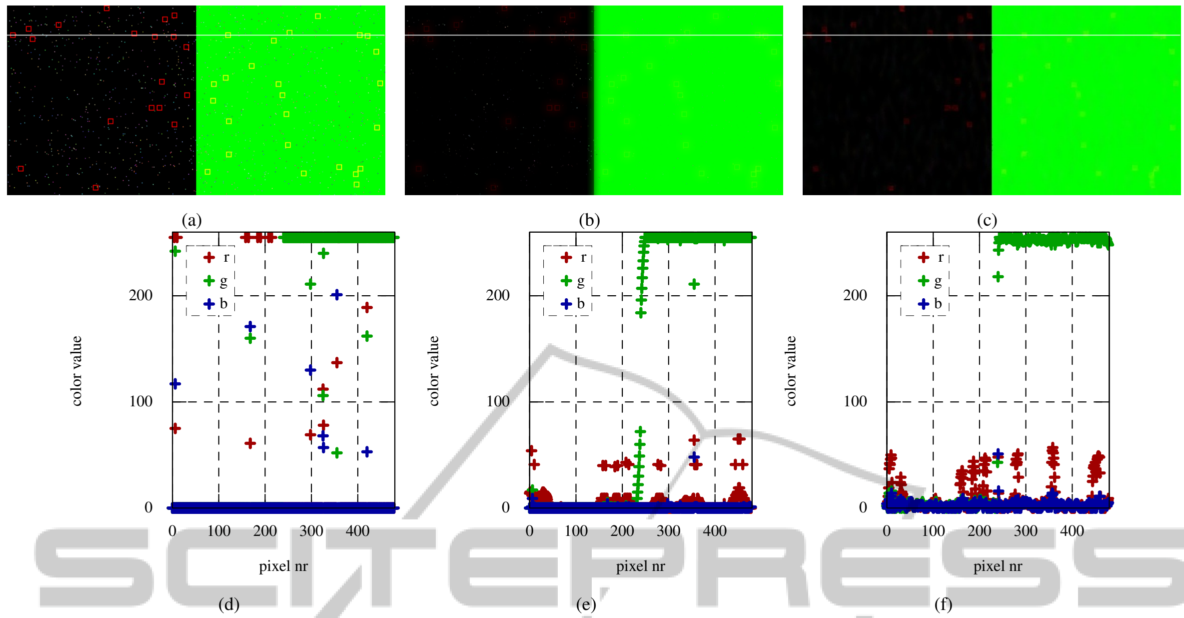

Figure 4: 4(a) Artificial input image with three features: a green color edge, texture is simulated using red squares 7 px wide, and white noise is added. A cross section is shown in white and can be seen in figure 4(d). 4(b) Bilateral Filter. For an arbitrary large kernel of 20 px in the space domain and using $\sigma_c = 200$ for the color domain all texture and noise is filtered. The color edge now has a width of 18 px. A cross section can be seen in figure 4(e). 4(c) Proposed texture filter. The edge remains sharp and all texture, as well as noise is smoothed out. A cross section can be seen in figure 4(f). 4(d) Cross section of original image. A green color step, as well as texture and noise can be seen. 4(e) Cross section of the bilateral filter. The color edge is not preserved, texture is removed, but some noise remains. 4(f) Cross section of proposed filter. The green color edge is preserved and texture, as well as all noise is removed.

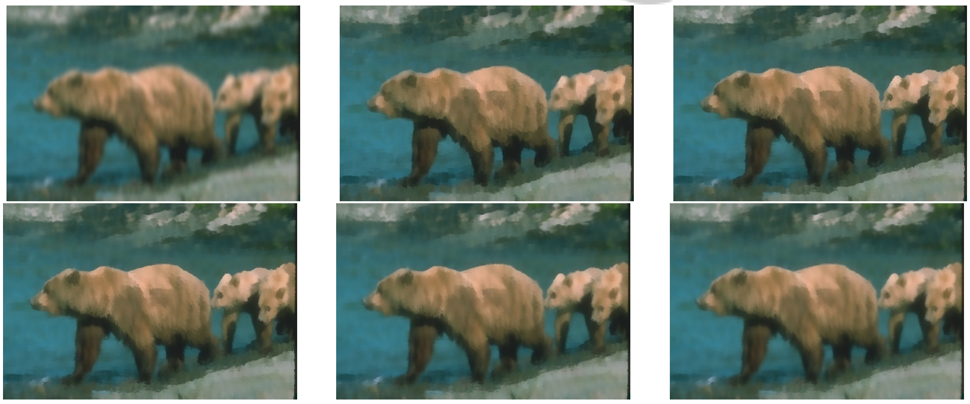

Figure 5: Effect of different thresholds. For low thresholds the image is more blurred, after $\tau = 30$ it does not change much. From top left to bottom right: $\tau = 5,\ 20,\ 30,\ 40,\ 60,\ 80$.

did not combine the mean-shift and the graph-based algorithm with the proposed filter, because both algorithms already perform their own preprocessing.

A visual comparison can be seen in figure 7. The proposed filter greatly reduces noise and texture and achieves a good trade-off between over- and under-segmentation as compared to the other methods. A comparison for a video sequence using the metropolis algorithm may be seen in figure 8. Labels are kept during the sequence and are encoded using different colors: both mean-shift and graph based segmentation do not use fixed label numbers for objects. The filter reduces the over-segmentation in textured areas, e.g. the suitcases, the pad, or the plant.

For robotic applications it is very important that the labels of image segments do not change throughout a video stream. Currently only very few segmentation algorithms running in real-time do achieve this (Abramov, 2012), among them the Metropolis algorithm.

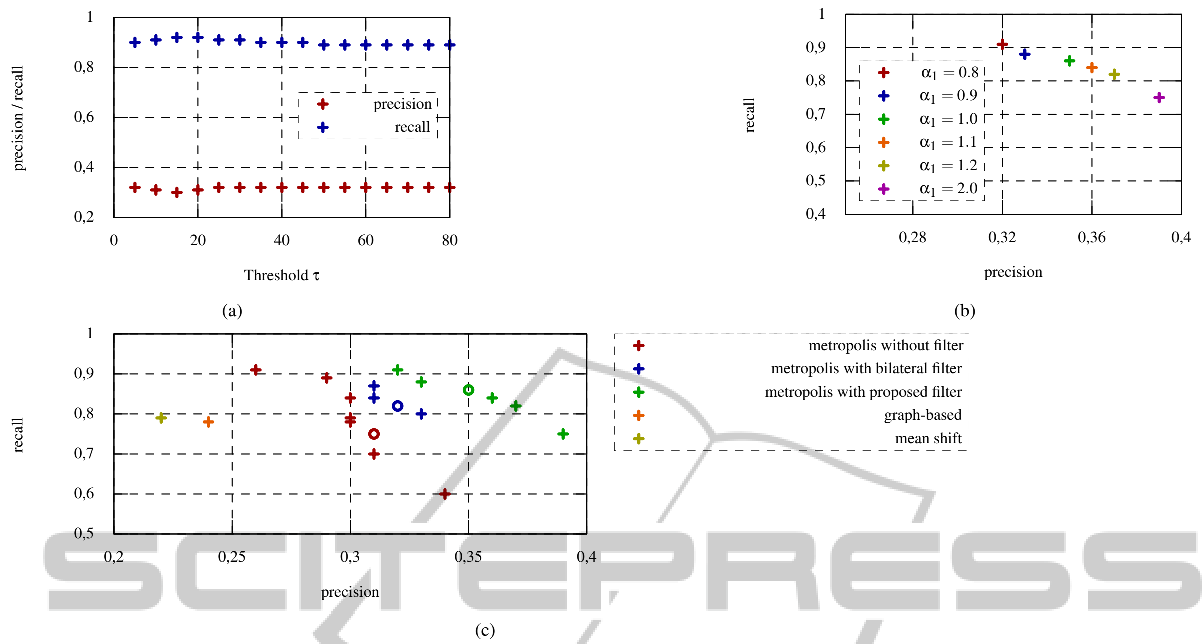

Figure 6: 6(a) Metropolis algorithm performance with fixed parameters using filtered images for various thresholds. 6(b) Estimating best segmentation parameters for a fixed threshold $\tau = 30$ using filtered images. 6(c) Comparison between graph-based, mean shift and Metropolis algorithm. Metropolis segmentation using $\alpha_1 = 1.0$ is marked with a circle.

3.3 Time Performance Results

We computed the average frame rates for images of different sizes in table 1. For comparison purposes, images from the Berkeley Segmentation Dataset and Benchmark were used (Martin et al., 2001). As shown in section 2 the complexity is independent of the threshold used. You can see that the GPU version is roughly 30 times faster than the CPU approach, independent of the image size. For images of size 480×320 px real-time processing of movies is achieved.

Table 1: Time performance for images of different sizes. The test image was taken from the training set of the Berkeley Segmentation Dataset and Benchmark (Martin et al., 2001) and is also used in figure 3(b). 100 measurements were taken and averaged.

Image Size	CPU		GPU	
[px]	[Hz]	[s]	[Hz]	[ms]
240×180	3.03	0.33	80.38	12.4
320×240	1.66	0.60	48.00	20.8
480×320	0.80	1.25	23.81	42.0
640×480	0.40	2.50	12.35	81.0
800×600	0.24	4.17	7.65	130.7
1024×768	0.15	6.67	4.24	235.9

4 CONCLUSIONS

In this paper, we presented a novel real-time edge preserving smoothing filter, which replaces noisy and textured areas by uniformly colored patches. The performance of a recent image segmentation method could be significantly improved using the filtered images. The time performance makes the filter applicable to video streams, as shown in figure 8, and hence can be used in the future as a component inside the perception-action loop of robotic applications. The proposed method improves the precision and recall trade-off of obtained segmentations. Furthermore, the detected features could be used for classification purposes in other applications.

ACKNOWLEDGEMENTS

The research leading to these results has received funding from the European Community's Seventh Framework Programme FP7/2007-2013 (Specific Programme Cooperation, Theme 3, Information and Communication Technologies) under grant agreement no. 269959, Intellact. B. Dellen acknowledges support from the Spanish Ministry of Science and Innovation through a Ramon y Cajal program.

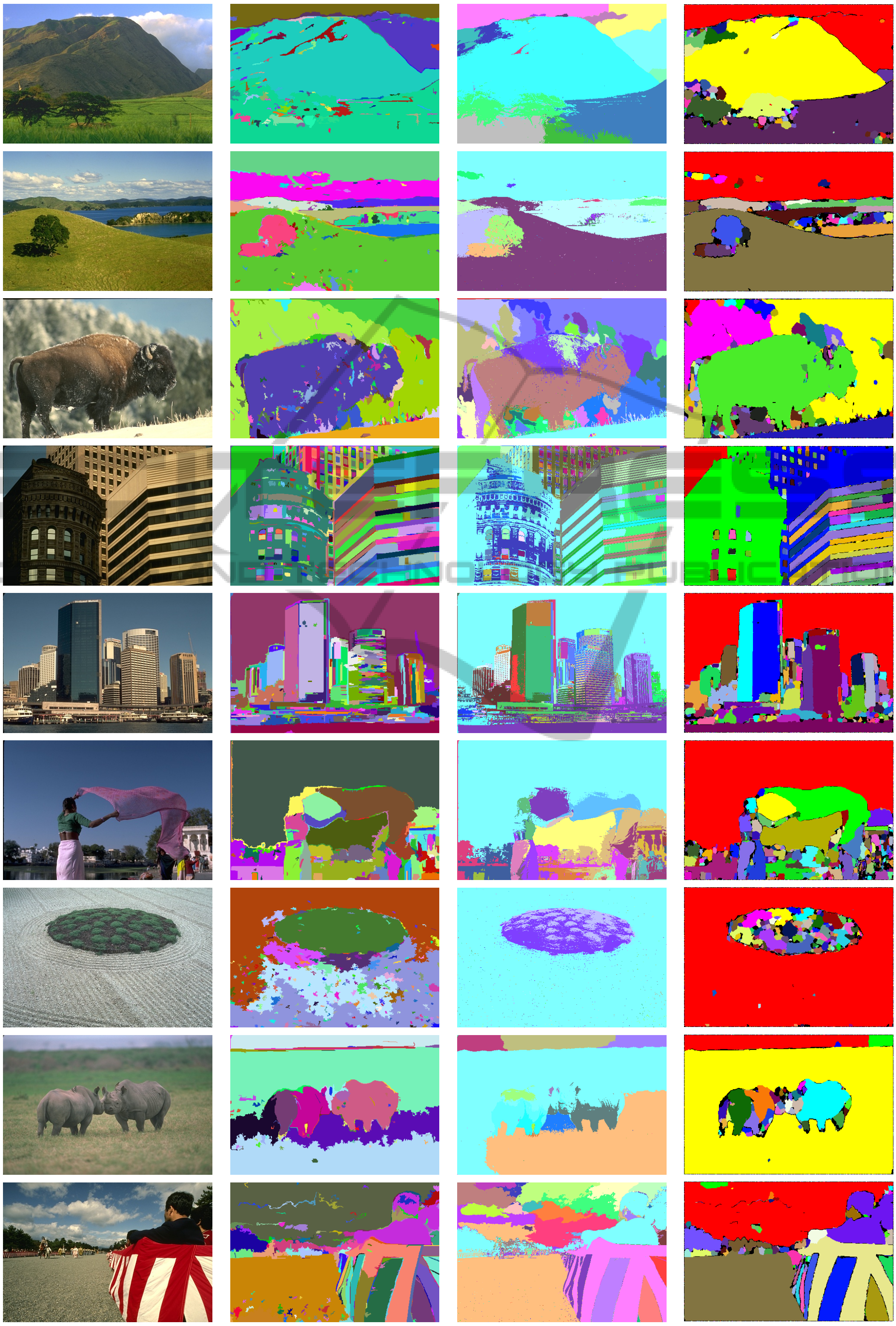

(a) (b) (c) (d)

Figure 7: Visual comparison of several threshold levels. 7(a) Original image. 7(b) Graph based segmentation. 7(c) Mean-shift segmentation. 7(d) Proposed filter in connection with metropolis algorithm.

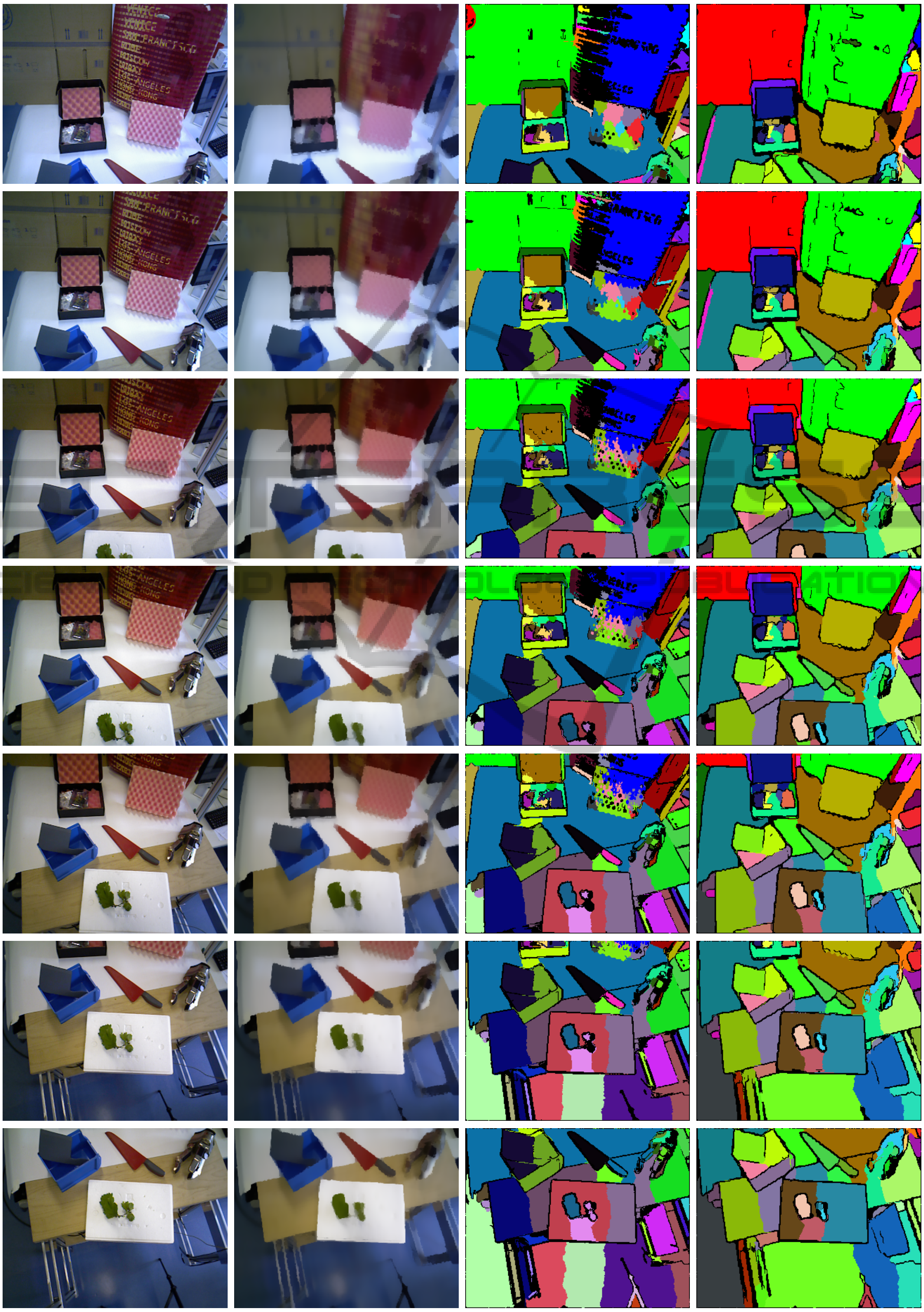

(a) (b) (c) (d)

Figure 8: Visual comparison of a short video sequence. 8(a) Original frames from sequence. 8(b) Filtered frames from sequence using the proposed filter. 8(c) Segmentation using the Metropolis algorithm without filter. 8(d) Segmentation using the Metropolis algorithm and the proposed filter. There is significant less over-segmentation in textured areas (e.g. suitcase, pad).

REFERENCES

Abramov, A. (2012). *Compression of the visual data into symbol-like descriptors in terms of the cognitive real-time vision system*. PhD thesis, Georg-August-Universität Göttingen.

Abramov, A., Pauwels, K., Papon, J., Wörgötter, F., and Dellen, B. (2012). Real-time segmentation of stereo videos on a portable system with a mobile gpu. *IEEE Transactions on Circuits and Systems for Video Technology*.

Cigla, C. and Aydin Alatan, A. (2008). Depth assisted object segmentation in multi-view video. In *3DTV Conference: The True Vision - Capture, Transmission and Display of 3D Video, 2008*, pages 185 –188.

Comaniciu, D. and Meer, P. (2002). Mean shift: a robust approach toward feature space analysis. *IEEE Transactions on Pattern Analysis and Machine Intelligence*, 24(5):603 –619.

Du, W., Tian, X., and Sun, Y. (2011). A dynamic threshold edge-preserving smoothing segmentation algorithm for anterior chamber oct images based on modified histogram. In *4th International Congress on Image and Signal Processing (CISP)*, volume 2, pages 1123 –1126.

Durand, F. and Dorsey, J. (2002). Fast bilateral filtering for the display of high-dynamic-range images. *ACM Trans. Graph.*, 21(3):257–266.

Elad, M. (2002). On the origin of the bilateral filter and ways to improve it. *IEEE Transactions on Image Processing*, 11(10):1141 – 1151.

Farbman, Z., Fattal, R., Lischinski, D., and Szeliski, R. (2008). Edge-preserving decompositions for multi-scale tone and detail manipulation. *ACM Trans. Graph.*, 27(3):67:1–67:10.

Farmer, M. and Jain, A. (2005). A wrapper-based approach to image segmentation and classification. *IEEE Transactions on Image Processing*, 14(12):2060 –2072.

Farsiu, S., Elad, M., and Milanfar, P. (2006). Multiframe demosaicing and super-resolution of color images. *IEEE Transactions on Image Processing*, 15(1):141 –159.

Felzenszwalb, P. and Huttenlocher, D. (2004). Efficient graph-based image segmentation. *International Journal of Computer Vision*, 59:167–181.

Jiang, W., Baker, M. L., Wu, Q., Bajaj, C., and Chiu, W. (2003). Applications of a bilateral denoising filter in biological electron microscopy. *Journal of Structural Biology*, 144(1–2):114 – 122.

Lev, A., Zucker, S. W., and Rosenfeld, A. (1977). Iterative enhancemnent of noisy images. *IEEE Transactions on Systems, Man and Cybernetics*, 7(6):435 –442.

Martin, D., Fowlkes, C., and Malik, J. (2004). Learning to detect natural image boundaries using local brightness, color, and texture cues. *IEEE Transactions on Pattern Analysis and Machine Intelligence*, 26(5):530 –549.

Martin, D., Fowlkes, C., Tal, D., and Malik, J. (2001). A database of human segmented natural images and its application to evaluating segmentation algorithms and measuring ecological statistics. In *Proc. 8th Int'l Conf. Computer Vision*, volume 2, pages 416–423.

Muneyasu, M., Maeda, T., Yako, T., and Hinamoto, T. (1995). A realization of edge-preserving smoothing filters using layered neural networks. In *IEEE International Conference on Neural Networks, Proceedings.*, volume 4, pages 1903 –1906 vol.4.

Paris, S. and Durand, F. (2007). A topological approach to hierarchical segmentation using mean shift. In *IEEE Conference on Computer Vision and Pattern Recognition (CVPR)*, pages 1 –8.

R., R. and W., S. (2003). Adaptive demosaicking. *J. Electron. Imaging*, 12(12):633.

Sun, D., Roth, S., and Black, M. (2010). Secrets of optical flow estimation and their principles. In *IEEE Conference on Computer Vision and Pattern Recognition (CVPR)*, pages 2432 –2439.

Tomasi, C. and Manduchi, R. (1998). Bilateral filtering for gray and color images. In *Sixth International Conference on Computer Vision*, pages 839 –846.

Xiao, J., Cheng, H., Sawhney, H., Rao, C., and Isnardi, M. (2006). Bilateral filtering-based optical flow estimation with occlusion detection. In Leonardis, A., Bischof, H., and Pinz, A., editors, *Computer Vision – ECCV 2006*, volume 3951 of *Lecture Notes in Computer Science*, pages 211–224. Springer Berlin / Heidelberg.

Yang, Q., Wang, S., and Ahuja, N. (2010). Svm for edge-preserving filtering. In *IEEE Conference on Computer Vision and Pattern Recognition (CVPR)*, pages 1775 – 1782.